Acta Crystallographica Section F
Structural Biology and Crystallization Communications
ISSN 1744-3091
Editors: **H. M. Einspahr and M. S. Weiss**

Crystallization and preliminary X-ray crystallographic analysis of an ice-binding protein (FfIBP) from *Flavobacterium frigoris* PS1

Hackwon Do, Jun Hyuck Lee, Sung Gu Lee and Hak Jun Kim

Acta Cryst. (2012). F**68**, 806–809

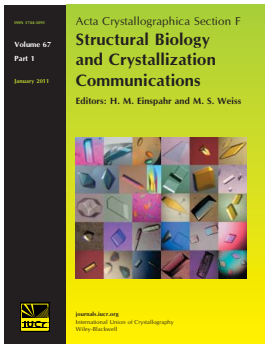

Acta Crystallographica Section F
Structural Biology and Crystallization Communications
ISSN 1744-3091

Crystallization and preliminary X-ray crystallographic analysis of an ice-binding protein (FfIBP) from *Flavobacterium frigoris* PS1

Hackwon Do,[a,b]‡ Jun Hyuck Lee,[a,b]‡ Sung Gu Lee[a,b] and Hak Jun Kim[a,b]*

[a]Division of Polar Life Sciences, Korea Polar Research Institute, Incheon 406-840, Republic of Korea, and [b]Department of Polar Sciences, University of Science and Technology, Incheon 406-840, Republic of Korea

‡ These authors contributed equally to this work.

Correspondence e-mail: hjkim@kopri.re.kr

Received 21 March 2012
Accepted 7 May 2012

Ice growth in a cold environment is fatal for polar organisms, not only because of the physical destruction of inner cell organelles but also because of the resulting chemical damage owing to processes such as osmotic shock. The properties of ice-binding proteins (IBPs), which include antifreeze proteins (AFPs), have been characterized and IBPs exhibit the ability to inhibit ice growth by binding to specific ice planes and lowering the freezing point. An ice-binding protein (FfIBP) from the Gram-negative bacterium *Flavobacterium frigoris* PS1, which was isolated from the Antarctic, has recently been overexpressed. Interestingly, the thermal hysteresis activity of FfIBP was approximately 2.5 K at 50 µ*M*, which is ten times higher than that of the moderately active IBP from Arctic yeast (LeIBP). Although FfIBP closely resembles LeIBP in its amino-acid sequence, the antifreeze activity of FfIBP appears to be much greater than that of LeIBP. In an effort to understand the reason for this difference, an attempt was made to solve the crystal structure of FfIBP. Here, the crystallization and X-ray diffraction data of FfIBP are reported. FfIBP was crystallized using the hanging-drop vapour-diffusion method with 0.1 *M* sodium acetate pH 4.4 and 3 *M* sodium chloride as precipitant. A complete diffraction data set was collected to a resolution of 2.9 Å. The crystal belonged to space group $P4_122$, with unit-cell parameters $a = b = 69.4$, $c = 178.2$ Å. The asymmetric unit contained one monomer.

1. Introduction

Many plants, insects, animals and other organisms have evolved unique adaptive mechanisms that allow them to survive in harsh environments with extreme temperatures (Rothschild & Mancinelli, 2001). To survive in extremely cold environments, many organisms produce antifreeze proteins (AFPs) and ice-binding proteins (IBPs). These proteins can lower the freezing point of a solution non-colligatively without affecting the melting point of the solution (thermal hysteresis); thus, the freezing of body fluids can be prevented. In addition, these proteins can inhibit ice recrystallization, where large ice crystals grow at the expense of smaller ones, thus preventing cell damage during freeze–thaw cycles (Knight *et al.*, 1984, 1991). It is generally accepted that these proteins function through adsorption of their flat ice-binding surfaces onto particular planes of ice crystals, thus preventing or inhibiting further ice growth (Yeh & Feeney, 1996). Notably, the antifreeze activities of AFPs and IBPs vary and depend on the protein structure. Therefore, structural studies are essential to understand the antifreeze and ice-binding mechanisms of these proteins.

AFPs are characterized according to their structure and their thermal hysteresis (TH) values and have been categorized into several types: types I–IV from fish, insect AFPs, bacterial AFPs and plant AFPs (Griffith *et al.*, 1997; Davies & Hew, 1990; Graether *et al.*, 2000). Recently identified IBPs from bacteria, diatoms and fungi form a distinct cluster according to phylogenetic analysis (Raymond & Janech, 2009). The first ice-active fungal protein was found in a snow mould, *Typhula ishikariensis* (Hoshino *et al.*, 2003), and similar ice-binding proteins were subsequently found in sea-ice diatoms (Janech *et al.*, 2006), a sea-ice bacterium (Raymond *et al.*, 2007), a bacterium from a deep ice core in the Antarctic ice sheet (Raymond *et al.*, 2008) and the Arctic yeast *Leucosporidium* sp. AY30 (Lee *et al.*, 2010).

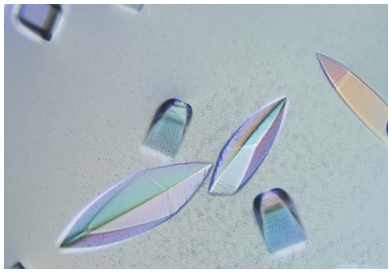

Recently, the crystal structure of IBP (LeIBP) from *Leucosporidium* sp. AY30 was determined in our laboratory. Structural and functional analyses of LeIBP have shown that this protein has a β-helical fold similar to those of insect and bacterial AFPs. However, the ice-binding site of LeIBP is more complex and does not have a simple ice-binding motif. Insect and bacterial AFPs use a Thr-*X*-Thr motif and a Thr-*X*-Asx motif, respectively, located in a flat β-sheet to bind ice (Lee *et al.*, 2012).

In this study, we succeeded in expressing and purifying an IBP (FfIBP) from an Antarctic bacterium, *Flavobacterium frigoris* PS1, isolated from sea ice on the shore of McMurdo Sound. The ice-binding property of FfIBP has previously been confirmed by ice-pitting experiments (Raymond *et al.*, 1989). FfIBP shows 56% amino-acid sequence similarity and 39% identity to LeIBP. However, FfIBP has up to a tenfold higher antifreeze activity compared with LeIBP. To determine the reason for this difference in activity, we performed structural and functional studies. We report the results of preliminary X-ray crystallographic experiments on FfIBP, which are the first step towards structural elucidation of FfIBP.

2. Materials and methods

2.1. Cloning, expression and purification of recombinant FfIBP

The FfIBP gene (amino acids 29–276), excluding the signal peptide sequence (amino acids 1–23) identified by *SignalP* (Petersen *et al.*,

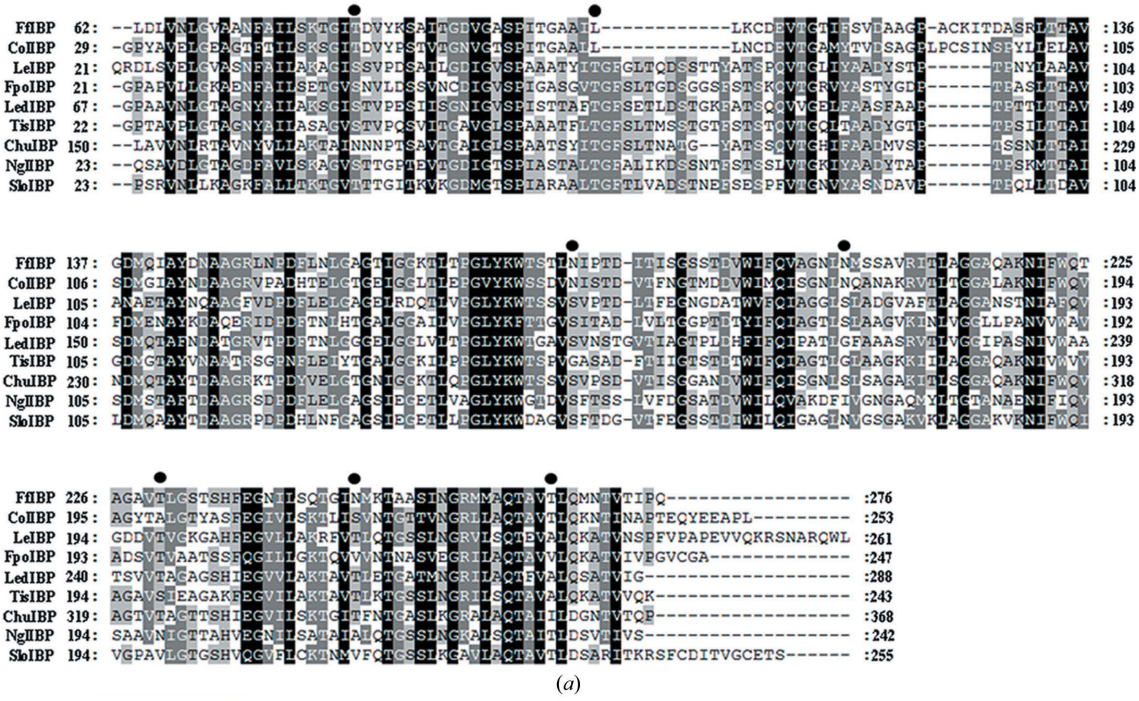

Figure 1
Multiple sequence alignment and antifreeze activity of recombinant FfIBP. (*a*) Sequence alignment of FfIBP and other IBPs from *Colwellia psychrerythraea* (ColIBP), *Leucosporidium* sp. AY30 (LeIBP), *Flammulina populicola* (FpoIBP), *Lentinula edodes* (LedIBP), *Typhula ishikariensis* (TisIBP), *Cytophaga hutchinsonii* ATCC 33406 (ChuIBP), *Navicula glaciei* (NglIBP) and *Stephos longipes* (SloIBP) using *ClustalX*. The residues constituting the ice-binding sites in the LeIBP structure are indicated by filled circles. Highly conserved residues are shaded grey and black. (*b*) An aliquot of purified FfIBP was visualized by 12% SDS–PAGE. (*c*) Comparison of the thermal hysteresis activities of FfIBP and LeIBP. The thermal hysteresis activity of FfIBP (circles) observed was 2.5 K at 50 μ*M*, which was approximately ten times greater than the activity of LeIBP (triangles).

2011), was amplified by polymerase chain reaction (PCR) using *F. frigoris* PS1 genomic DNA as a template. The forward primer was 5′-CGA TAA CAT ATG TCT CTA TCA GTT GCA AAT-3′ and the reverse primer was 5′-CGA TAA CTC GAG TCA TTG TGG TAT GGT AAC GGT-3′. Amplified fragments were cleaved with *Nde*I and *Xho*I and cloned into the pCold I vector (Takara Bio Inc., Japan) to produce a factor Xa protease-cleavable N-terminally 6×His-tagged fusion protein. The construct was verified by DNA sequencing and transformed into *Escherichia coli* strain BL21 (DE3) for expression. The cells were grown in LB medium at 310 K in the presence of 100 µg ml^{-1} ampicillin until the OD_{600} approached 0.6. Recombinant protein expression was then induced using 1 m*M* isopropyl *β*-D-1-thiogalactopyranoside (IPTG) at 289 K for 24 h. The cell pellet was harvested by centrifugation and resuspended in cold lysis buffer consisting of 50 m*M* sodium phosphate pH 8.5, 300 m*M* NaCl, 5 m*M* imidazole, 0.5 mg ml^{-1} lysozyme, 1 m*M* phenylmethylsulfonyl fluoride (PMSF). After 30 min incubation at 277 K, the cells were disrupted by ultrasonication (Vibra-Cell VCX400). The lysate was centrifuged again at 16 000 rev min^{-1} for 40 min at 277 K to remove cell debris and the supernatant was poured into a His-tag affinity column. The bound FfIBP was washed with ten column volumes of lysis buffer and eluted with elution buffer consisting of 50 m*M* sodium phosphate pH 8.5, 300 m*M* NaCl, 300 m*M* imidazole. After cleavage of the 6×His tag at 277 K overnight, size-exclusion chromatography was performed as the next step of purification. The sample was applied onto a Superdex 200 HiLoad 16/60 column equilibrated with 20 m*M* Tris–HCl pH 8.5, 150 m*M* NaCl.

2.2. Antifreeze activity (thermal hysteresis) assay

Measurement of the thermal hysteresis (TH) activity was performed as described previously (Lee *et al.*, 2012). Briefly, the sample was placed on the surface of a temperature-controlled metal block and cooled rapidly to around 253 K using a nanolitre osmometer (Otago Osmometers, Dunedin, New Zealand) equipped with a Canon digital camera (PowerShot A620). After 5 min incubation, the temperature was raised slowly to obtain a single ice crystal. When only one ice crystal remained, the temperature was slowly lowered again (−0.5 K min^{-1}). The freezing point of the sample was taken as the temperature at which there was rapid ice-crystal growth. The TH value was defined as the maximum difference between the melting and freezing temperatures of the sample. The ice-crystal morphology produced by IBPs in distilled water was examined.

2.3. Crystallization and data collection

Purified FfIBP was concentrated to 16.4 mg ml^{-1} and crystallized by the hanging-drop vapour-diffusion method at 293 K. The drops consisted of 1 µl protein solution (16.4 mg ml^{-1} protein in 20 m*M* Tris–HCl pH 8.5, 150 m*M* NaCl) and 1 µl reservoir solution (0.1 *M* sodium acetate pH 4.4, 3 *M* sodium chloride). A single crystal formed after 2 d and grew to a largest dimension of 0.5 mm. Successful flash-cooling was achieved when the FfIBP crystals were transferred directly into Paratone oil and allowed to equilibrate for 2 min. Native data for FfIBP were collected to a resolution of 2.9 Å using the X-ray facility home source at the Korea Basic Science Institute (KBSI), Ochang, Republic of Korea. The data were processed using *iMOSFLM* and *SCALA* (Battye *et al.*, 2011).

The crystals belonged to space group $P4_122$, with unit-cell parameters $a = b = 69.4$, $c = 178.2$ Å. The phases were determined by molecular replacement using *MOLREP* with the coordinates of the LeIBP structure (PDB entry 3uyu; Lee *et al.*, 2012). After computational refinement using *REFMAC*5 (Murshudov *et al.*, 2011), an interpretable electron-density map was calculated in *CCP*4 (Winn *et al.*, 2011). Model building using *Coot* (Emsley & Cowtan, 2004) and further refinement is under way.

3. Results and discussion

An ice-binding protein (FfIBP) from *F. frigoris* PS1 was cloned, overexpressed and purified in *E. coli* BL21 (DE3) cells (Figs. 1*a* and 1*b*). Purified FfIBP appeared to be a monomer as suggested by the size-exclusion chromatography elution profile and the results of analytic ultracentrifugation (data not shown). In the LeIBP structure a C-terminal hydrophobic loop adopts an extended conformation and plays in a role in dimer formation (Lee *et al.*, 2012). However, this C-terminal region is not present in FfIBP, which may cause FfIBP to behave as a monomer in solution. Notably, C-terminally truncated LeIBP had a greater TH activity than the wild-type protein. We had predicted that removal of the C-terminus would prevent the interactions necessary for dimerization, allowing the protein to be freely accessible for ice binding in the monomeric state. The monomeric state may confer higher TH activity on the C-terminally truncated LeIBP mutant. Most strikingly, the recombinant FfIBP displayed a

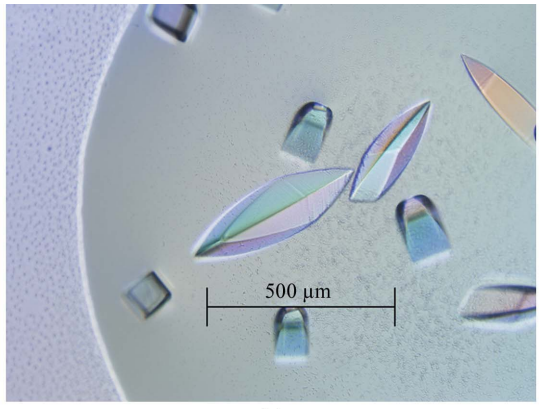

(*a*)

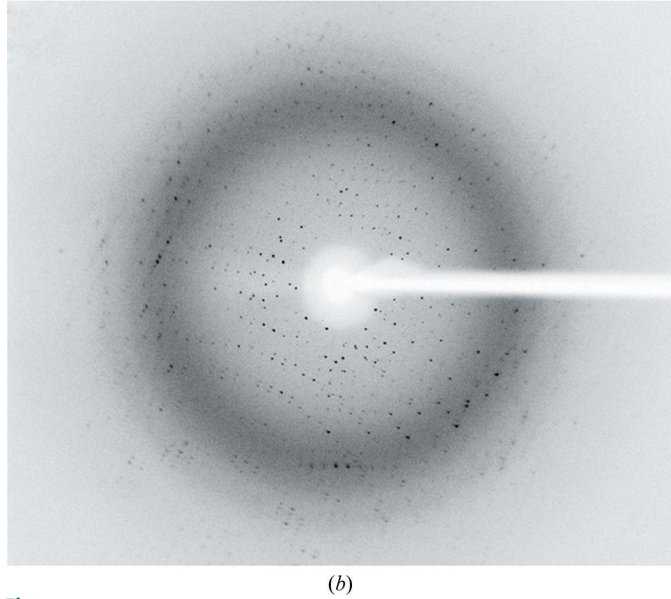

(*b*)

Figure 2
Crystal morphology and diffraction pattern of recombinant FfIBP. (*a*) FfIBP crystals grown in 0.1 *M* sodium acetate pH 4.4, 3 *M* sodium chloride. (*b*) X-ray diffraction image (2.9 Å resolution) obtained during data collection from the FfIBP crystal.

Table 1
Data-collection statistics.

Values in parentheses are for the highest resolution shell.

X-ray source	Rigaku MicroMax-007 HF at KBSI
Space group	$P4_122$
Unit-cell parameters (Å)	a = 69.4, b = 69.4, c = 178.2
Wavelength (Å)	1.5418
Resolution range (Å)	69.36–2.90 (3.06–2.90)
No. of observed reflections	74340 (9447)
No. of unique reflections	10314 (1458)
Completeness (%)	99.9 (100)
Multiplicity	7.2 (6.5)
$R_{\rm merge}$†	0.147 (0.405)
$\langle I/\sigma(I)\rangle$	9.0 (3.0)

† $R_{\rm merge} = \sum_{hkl}\sum_i |I_i(hkl) - \langle I(hkl)\rangle| / \sum_{hkl}\sum_i I_i(hkl)$, where $I_i(hkl)$ is the intensity of the ith observation of reflection hkl, $\sum_{hkl}$ is the sum over all reflections and $\sum_i$ is the sum over i measurements of reflection hkl.

TH activity of 2.5 K at 50 µ*M*, which is ten times greater than the activity of the moderately active LeIBP (0.17 K at 50 µ*M*; Fig. 1*c*; Lee *et al.*, 2012). Although FfIBP shares protein sequence similarity with LeIBP and is expected to have a similar overall three-dimensional structure, it exhibits distinct differences from LeIBP, including differences in oligomerization state and TH activity.

To obtain structural information about the mechanisms responsible for the hyper-antifreeze activity and the differences in the ice-binding mechanism of FfIBP, we performed X-ray crystallography experiments. Purified FfIBP was concentrated to 16.4 mg ml^{-1} and quadrangular pyramid-shaped crystals suitable for diffraction (maximum dimension of 500 µm; Fig. 2*a*) were grown in 0.1 *M* sodium acetate pH 4.4, 3 *M* sodium chloride. Complete diffraction data were collected to a resolution of 2.9 Å (Fig. 2*b*). The crystal belonged to space group $P4_122$, with unit-cell parameters $a = b = 69.4$, $c = 178.2$ Å (Table 1). The Matthews coefficient ($V_{\rm M}$) of 4.21 Å^3 Da^{-1} suggests the presence of one molecule in the asymmetric unit, with a solvent content of 70.8% (Matthews, 1968). A good molecular-replacement solution (translation-function contrast value of 18.8 and *R* factor of 48%) was obtained using the monomeric model of the LeIBP structure (PDB entry 3uyu) with the *MOLREP* software. The resulting PDB file was refined against the original data set in *REFMAC*5 (Murshudov *et al.*, 2011) and had reasonable $R_{\rm work}$ and $R_{\rm free}$ values of 25.5% and 32.3%, respectively. Further structure refinement and model building of FfIBP are currently in progress; the structural details will be reported elsewhere.

We thank the staff at the X-ray core facility of the Korea Basic Science Institute (KBSI), Ochang, Republic of Korea. This work was supported by the National Agenda Project of the Korea Research Council of Fundamental Science and Technology (KRCF; grant No. PG11010 to HJK) and the Korea Polar Research Institute (KOPRI; grant Nos. PE11100 to HJK and PE11120 to JHL).

References

Battye, T. G. G., Kontogiannis, L., Johnson, O., Powell, H. R. & Leslie, A. G. W. (2011). *Acta Cryst.* D**67**, 271–281.
Davies, P. L. & Hew, C. L. (1990). *FASEB J.* **4**, 2460–2468.
Emsley, P. & Cowtan, K. (2004). *Acta Cryst.* D**60**, 2126–2132.
Graether, S. P., Kuiper, M. J., Gagné, S. M., Walker, V. K., Jia, Z., Sykes, B. D. & Davies, P. L. (2000). *Nature (London)*, **406**, 325–328.
Griffith, M., Antikainen, M., Hon, W.-C., Pihakaski-Maunsbach, K., Yu, X.-M., Chun, J. U. & Yang, D. S. C. (1997). *Physiol. Plant.* **100**, 327–332.
Hoshino, T., Kiriaki, M., Ohgiya, S., Fujiwara, M., Kondo, H., Nishimiya, Y., Yumoto, I. & Tsuda, S. (2003). *Can. J. Bot.* **81**, 1175–1181.
Janech, M. G., Krell, A., Mock, T., Kang, J.-S. & Raymond, J. A. (2006). *J. Phycol.* **42**, 410–416.
Knight, C. A., Cheng, C. C. & DeVries, A. L. (1991). *Biophys. J.* **59**, 409–418.
Knight, C. A., DeVries, A. L. & Oolman, L. D. (1984). *Nature (London)*, **308**, 295–296.
Lee, J. H., Park, A. K., Do, H., Park, K. S., Moh, S. H., Chi, Y. M. & Kim, H. J. (2012). *J. Biol. Chem.* **287**, 11460–11468.
Lee, J. K., Park, K. S., Park, S., Park, H., Song, Y. H., Kang, S.-H. & Kim, H. J. (2010). *Cryobiology*, **60**, 222–228.
Matthews, B. W. (1968). *J. Mol. Biol.* **33**, 491–497.
Murshudov, G. N., Skubák, P., Lebedev, A. A., Pannu, N. S., Steiner, R. A., Nicholls, R. A., Winn, M. D., Long, F. & Vagin, A. A. (2011). *Acta Cryst.* D**67**, 355–367.
Petersen, T. N., Brunak, S., von Heijne, G. & Nielsen, H. (2011). *Nature Methods*, **8**, 785–786.
Raymond, J. A., Christner, B. C. & Schuster, S. C. (2008). *Extremophiles*, **12**, 713–717.
Raymond, J. A., Fritsen, C. & Shen, K. (2007). *FEMS Microbiol. Ecol.* **61**, 214–221.
Raymond, J. A. & Janech, M. G. (2009). *Cryobiology*, **58**, 151–156.
Raymond, J. A., Wilson, P. & DeVries, A. L. (1989). *Proc. Natl Acad. Sci. USA*, **86**, 881–885.
Rothschild, L. J. & Mancinelli, R. L. (2001). *Nature (London)*, **409**, 1092–1101.
Winn, M. D. *et al.* (2011). *Acta Cryst.* D**67**, 235–242.
Yeh, Y. & Feeney, R. E. (1996). *Chem. Rev.* **96**, 601–618.